Journal of Power Sources 196 (2011) 8000–8003

Contents lists available at ScienceDirect

Journal of Power Sources

journal homepage: www.elsevier.com/locate/jpowsour

Short communication

Amorphous CoSn alloys decorated by Pt as high efficiency electrocatalysts for ethanol oxidation

Hui Wang[a], Xiangtai Zhang[a], Rongfang Wang[a,*], Shan Ji[b], Wei Wang[a], Qizhao Wang[a], Ziqiang Lei[a,**]

[a] Key Laboratory of Eco-Environment-Related Polymer Materials, Ministry of Education of China, Key Laboratory of Gansu Polymer Materials, College of Chemistry and Chemical Engineering, Northwest Normal University, Lanzhou 730070, China
[b] South African Institute for Advanced Materials Chemistry, University of the Western Cape, 7535 Cape Town, South Africa

ARTICLE INFO

Article history:
Received 1 April 2011
Received in revised form 22 May 2011
Accepted 23 May 2011
Available online 30 May 2011

Keywords:
Electrocatalysts
Amorphous alloy
Ethanol oxidation
Low platinum

ABSTRACT

This study examines the electro-catalytic behaviour of Pt decorating amorphous alloys in the electro-oxidation of ethanol. Pt decorated CoSn nanoparticles on carbon (denoted as Pt-CoSn/C) are prepared using a two-stage chemical synthesis (sol–gel preparation and Steady-state replacement method). The structure of Pt-CoSn/C nanoparticles is confirmed by the transmission electron microscopy (TEM) and X-ray diffraction (XRD). Under the same quantity of platinum, the Pt-CoSn/C nanoparticles have higher activity in alcohol oxidation than the Pt/C, PtRu/C and PtSn/C nanoparticles in cyclic voltammetry tests. The structure of Pt decorating amorphous CoSn alloys notably decreases the usage of Pt and enhances its catalytic activity at the same time.

1. Introduction

Various recent studies have aimed at increasing the electrocatalytic activity and stability of platinum for the electro-oxidation of ethanol for fuel cell applications [1–4]. Among Pt-based binary catalysts, PtSn alloy has been reported as the most effective for the electro-oxidation of ethanol [5–12]. The promotional effect of Sn atoms for ethanol oxidation is related to the enhancement of CO oxidation rate by the bifunctional mechanism [13].

Compared to conventional crystalline metal, amorphous alloys can present unique compositions and surface structures for molecular reactions, which make them interesting materials in catalysis [14,15]. Stancheva et al. reported that the Fe- and Co-based amorphous alloys display catalytic activity for the oxidation of hydrogen and carbon monoxide [14]. Another active amorphous composition, Ni–S–Co also demonstrated high electrochemical activity and stability for hydrogen evolution reaction [16]. However, very little work has focused on the electrochemical characterization of methanol and ethanol oxidation on amorphous composition substrates [17].

A recent report by Zhang et al. on the catalytic oxidation of ammonia borane found that Fe@Pt nanoparticles with amorphous Fe cores generated a maximum current more than 3 times higher (up to 354%) than that of a commercial, crystalline Pt/C catalyst counterpart [18]. As far as we know, there are as yet no reports on the use of Pt decorated amorphous alloys for electrocatalytic oxidation of ethanol, and therefore the synthesis of carbon supported Pt decorating amorphous CoSn alloys and a study of their catalytic activities are of great interest.

In this paper, we introduce carbon supported platinum decorating amorphous CoSn alloys (Pt-CoSn/C) as an electrocatalyst, its preparation using a two-step reduction method, and test its ethanol oxidation activity and stability in acid media.

2. Experimental

2.1. Preparation of Pt-CoSn/C catalyst

Firstly, stannic chloride pentahydrate (148 mg) and cobaltous nitrate hexahydrate (253 mg) were dissolved in 20 mL ethylene glycol (EG) solution and ultrasonically treated for 0.5 h in a flask. Then, sodium citrate and sodium formate were dissolved in EG and stirred for 0.5 h. The pH was adjusted to 8–10 by addition of a 5 wt% KOH/EG solution with vigorous stirring. Vulcan XC-72R was added to the mixture under ultrasonic stirring. Consequently, the mixed solution heated at 453 K for 10 h. The resultant was washed with deionized water and dried at 323 K for 4 h. The CoSn/C nanoparticle was obtained.

Secondly, appropriate amounts of chloroplatinic acid (7 mg) aqueous solution were added to another flask and the pH was adjusted to 8–10 by addition of a 5 wt% KOH/H_2O solution. The

* Corresponding author. Tel.: +86 931 7971533; fax: +86 931 7971533.
** Corresponding author. Tel.: +86 931 7970359; fax: +86 931 7970359.
E-mail addresses: wrf38745779@126.com (R. Wang), leizq@nwnu.edu.cn (Z. Lei).

0378-7753/$ – see front matter © 2011 Elsevier B.V. All rights reserved.
doi:10.1016/j.jpowsour.2011.05.062

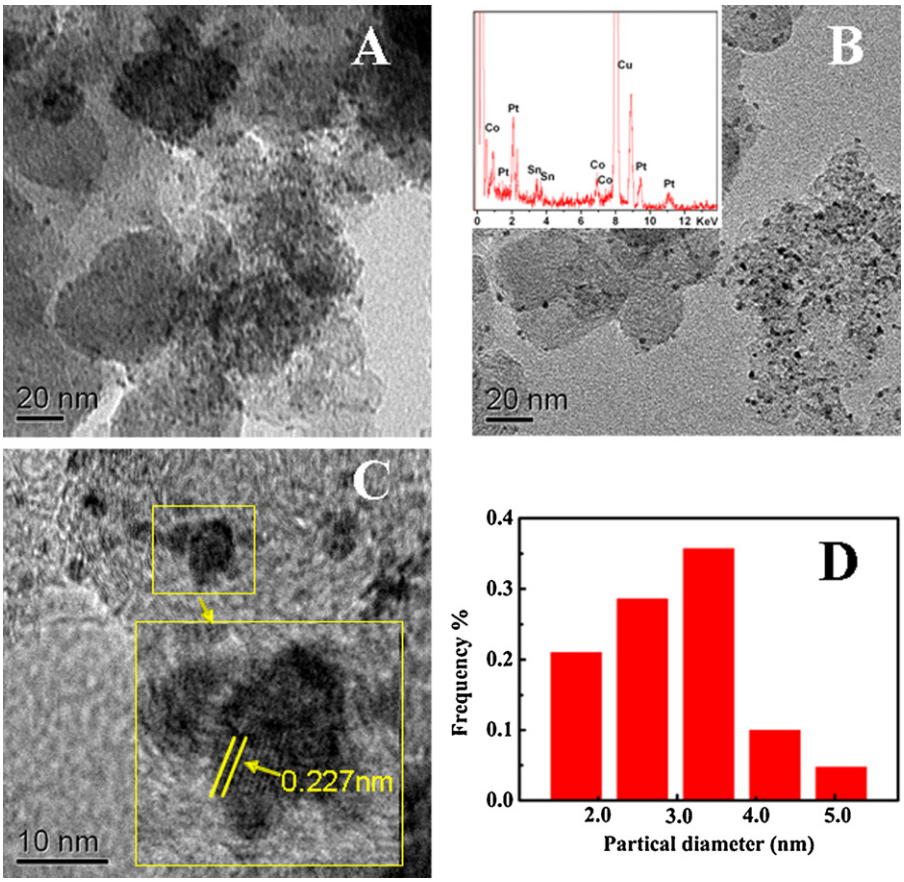

Fig. 1. TEM images of the CoSn/C (A) and Pt-CoSn/C (B) catalysts; HRTEM image of the Pt-CoSn/C catalysts (C); metal particle size distribution histogram of the Pt-CoSn/C catalyst (D); Inset: the EDX of Pt-CoSn/C (B).

obtained CoSn/C (50 mg) was submitted into the flask and the mixture was heated for 6 h at 353 K. The resultant was cooled and washed with deionized water. The Pt-CoSn/C catalyst was formed and dried at 323 K for 4 h. For comparison, PtSn/C (Atom ratio Pt:Sn = 3:1) were synthesized using the same method as CoSn/C and commercially available Pt/C (20 wt%) and PtRu/C (30 wt%, atom ratio 1:1) from J.M. Company were used.

2.2. Measurements

The catalysts were characterized by recording their XRD patterns on a Shimadzu XD-3A (Japan), using filtered Cu-Kα radiation. All X-ray diffraction patterns were analyzed using Jade 7.5 of Material Data, Inc. (MDI): peak profiles of individual reflections were obtained by a nonlinear least-square fit of the Cu Kα corrected data. TEM-measurements were carried out on a Tecnai G220 S-TWIN (FEI Company); the acceleration voltage was 200 kV. The energy-dispersive X-ray spectroscopy (EDX) analysis was performed in an analyzer associated with TEM.

The electrochemical measurements of catalysts were performed using an electrochemical work station (RST 3000). A common three-electrode electrochemical cell was used for the measurements. The counter and reference electrode were a platinum wire and an Ag/AgCl (3 M KCl) electrode, respectively. The working electrode was a glassy carbon disk (5 mm in diameter). The thin-film electrode was prepared as follows: 5 mg of catalyst was dispersed ultrasonically in 1 mL Nafion/ethanol (0.25% Nafion) for 15 min. 8 μL of the dispersion was transferred onto the glassy carbon disk using a pipette, and then dried in the air.

3. Results and discussion

Fig. 1 shows the TEM images of the CoSn/C and Pt-CoSn/C nanoparticles. CoSn and Pt-CoSn nanoparticles are highly dispersed on carbon support and do not aggregate. The average metal particle size of CoSn and Pt-CoSn is about 2.2 nm and 2.3 nm, respectively. There is no significant change with the average metal particle size from CoSn to Pt-CoSn. Fig. 1C displays a typical high resolution transmission electron microscopy (HRTEM) image of Pt-CoSn/C nanoparticle. The distance between two adjacent lattice planes is approximately 0.227 nm, which is close to the (1 1 1) interplanar distance of pure Pt (0.23 nm). It illustrates that the outer atoms of CoSn nanoparticles are Pt atoms. The EDX result of Pt-CoSn/C atomic ration of Pt:Co:Sn is 1:1:0.25 (Inserted in Fig. 1B).

XRD patterns of the CoSn/C, Pt-CoSn/C, PtSn/C and Pt/C are shown in Fig. 2. The Pt-CoSn/C, PtSn/C and Pt/C samples have the four main characteristic peaks of the face-centered cubic (fcc) crystalline Pt. In the case of PtSn/C sample, these diffraction peaks are shifted to higher 2θ values with respect to the corresponding peaks in the Pt/C sample. The shift of the peaks to higher angles reveals the alloy formation between Pt and Sn, which is caused by the incorporation of Sn in the fcc structure of Pt.

The XRD pattern of the CoSn sample shows that CoSn alloy is in the amorphous state. After Pt atoms were deposited on the metal particles, the XRD pattern of the sample changed significantly. We can observe that the peaks of the fcc crystalline Pt are clearly visible in the XRD pattern of the Pt-CoSn/C sample and do not have apparently shift compared to those of Pt/C sample, suggesting that Pt atoms occupy the surface of CoSn nanoparticles, rather than alloying with CoSn nanoparticles [18,19]. It is noted that Pt (1 1 1)

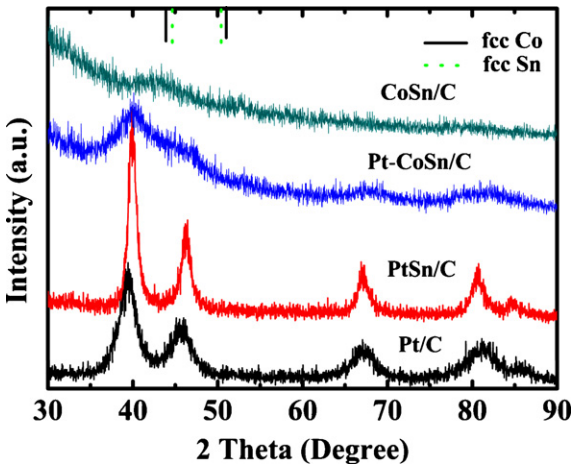

Fig. 2. The XRD patterns of CoSn/C, Pt-CoSn/C, PtSn/C and Pt/C.

diffraction angle of Pt-CoSn/C sample moves to slightly higher positions, indicating that PtCoSn alloy exists in the Pt-CoSn/C sample. The reason might be that the freshly reduced Pt atoms on the CoSn nanoparticles surface are very active, leading to the easy formation of PtCoSn alloy and occurrence of the Pt (1 1 1) diffraction peak shift in the XRD patterns [20].

The mean crystallize size of the particles can be calculated using DebyeeScherrer formula [21], the mean crystallize size of Pt-CoSn/C catalysts is ca. 3.3 nm, which is close to the TEM result.

The electrochemical properties of CoSn/C, Pt-CoSn/C, PtSn/C, PtRu/C and Pt/C have been investigated by cyclic voltammetry (CV). The corresponding results are present in Fig. 3. No hydrogen adsorption/desorption peaks are found in the curve of CoSn/C. This indicates CoSn/C has no contribution for the H desorption. Hydrogen adsorption-desorption peaks can be observed in the curve of Pt-CoSn/C, which indicates that Pt atoms are located on the electrocatalyst surface. Furthermore, the peak potential of the reduction of Pt-OH_{ad} is shifted negatively on the Pt-CoSn/C compared with those on other catalysts. It indicates that the Pt-CoSn/C show increased oxophilicity, a strengthened chemical adsorption energy with oxygen-containing species [22].

The electrochemical active surface area (ECSA) of the electrocatalyst can be calculated according to the equation [23]:

$$\mathrm{ECSA}\,(\mathrm{m^2\,g^{-1}}) = \frac{Q_H}{(2.1 \times [\mathrm{Pt}])}$$

where Q_H ($\mathrm{C\,m^{-2}}$) is the average integrated charge in the hydrogen adsorption/desorption peak area in the CV curves after subtracting the charge from the double-layer region, [Pt] ($\mathrm{g\,m^{-2}}$) is the Pt loading on the electrode, and 2.1 is the charge ($\mathrm{C\,m^{-2}}$) required to oxidize a monolayer of hydrogen on the Pt surface. The electrochemical surface areas (ECSA) are shown in Fig. 3B. The high ECSA for Pt-CoSn/C is favorable to electrochemical reaction toward ethanol oxidation.

As shown in Fig. 3C, the electrocatalytic activities for ethanol oxidation of CoSn/C, Pt-CoSn/C, PtSn/C, PtRu/C and Pt/C catalysts are investigated. The curve of CoSn/C shows that the CoSn/C sample has no electrocatalytic activity for ethanol oxidation. It can be observed that the mass activities of all peaks at the Pt-CoSn/C electrode are higher than those at the PtSn/C, PtRu/C and Pt/C electrodes. The mass activity and onset potential of Pt-CoSn/C, PtSn/C, PtRu/C and Pt/C catalyst for ethanol oxidation are shown in Fig. 3D. The lowest onset potential is obtained for the ethanol oxidation process using Pt-CoSn/C. The lower onset potential and higher mass activity of the Pt-CoSn/C for catalyst ethanol oxidation indicate that it is superior to the other catalysts.

There are four possible reasons for these results which originate from the structure and composition of the Pt-CoSn/C catalyst: (i) the Pt atoms are arranged on the surface of the metal particles, which could maximize the use of platinum atoms, resulting in the mass activity of the Pt-CoSn/C catalyst being much larger than others [24]; (ii) Sn increases the CO oxidation rate in bifunctional reaction

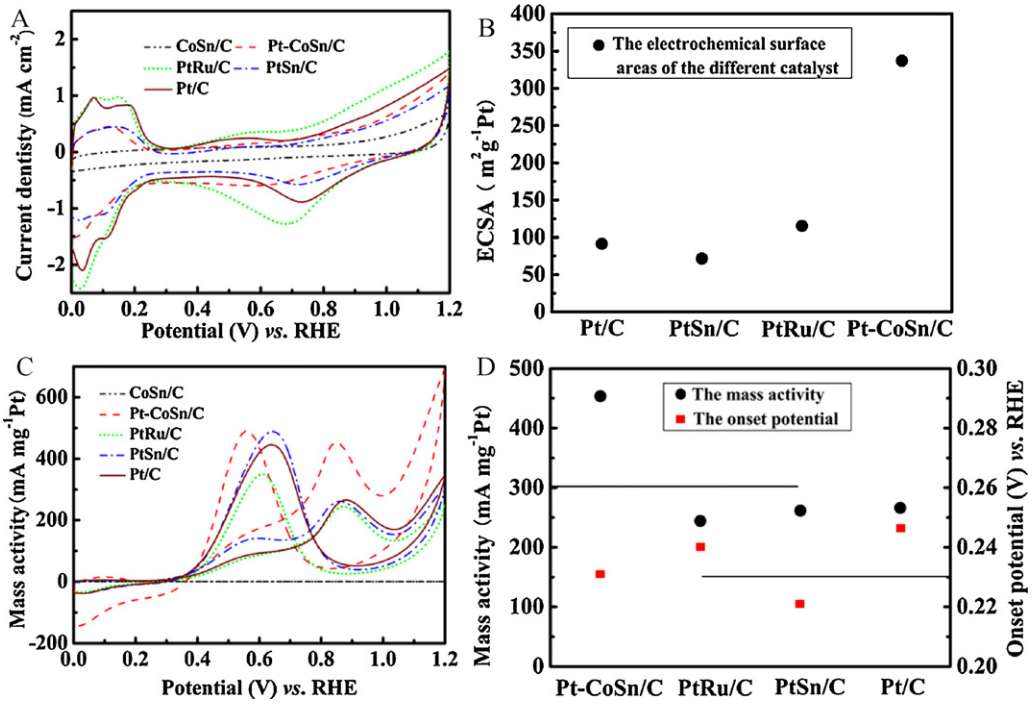

Fig. 3. Cyclic voltammograms of CoSn/C, Pt-CoSn/C, PtRu/C, PtSn/C and Pt/C catalysts in (A) 0.5 M H_2SO_4 normalized by the geometric electrode surface and (C) 0.5 M CH_3CH_2OH + 0.5 M H_2SO_4 solution under N_2 atmosphere normalized by the Pt mass in the catalysts; scan rate: 50 mV s^{-1}; (B) ECSAs calculated from hydrogen adsorption/desorption region; (D) the mass activity and onset potential from the CVs.

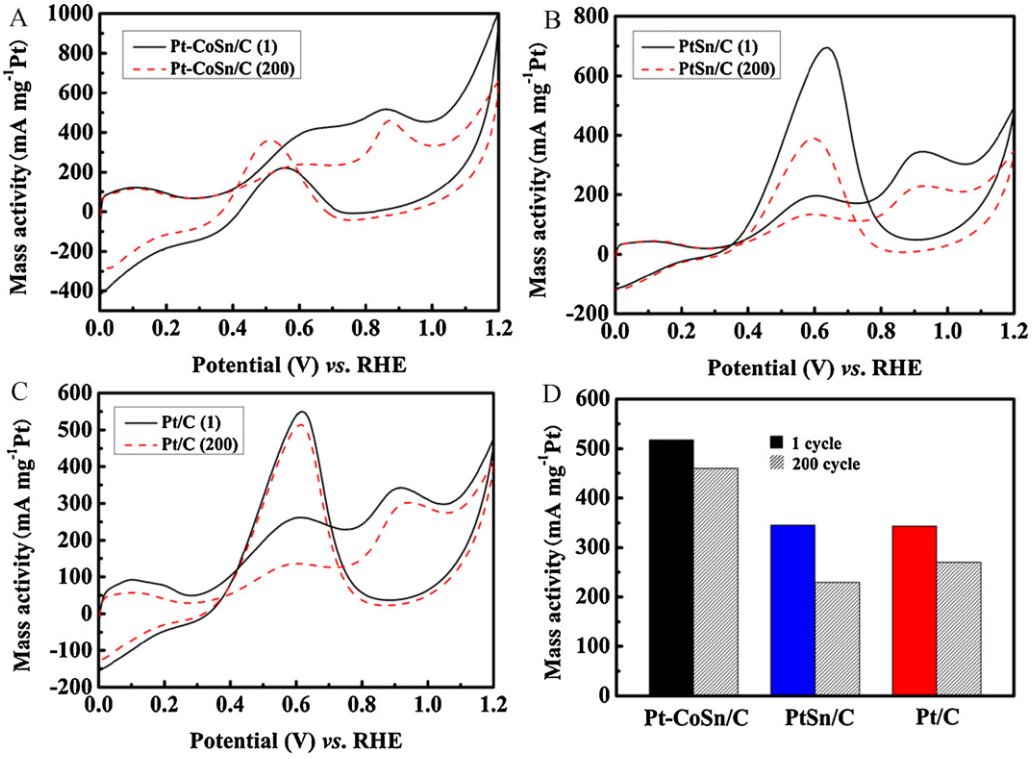

Fig. 4. The EOR mass activities of the Pt-CoSn/C (A), PtSn/C (B) and Pt/C (C) catalysts before and after 200 cycles in 0.5 M CH_3CH_2OH + 0.5 M H_2SO_4 solution under N_2 atmosphere; scan rate: 200 mV s^{-1}. (D) Histogram of stabilities of the catalysts.

mechanism operative for oxidation of CO on the Pt-CoSn/C catalyst [25,26]; (iii) CoSn alloys in the amorphous state hold many more lattice defects and thus could give birth to distinct effects in mediating the electronic structure and/or tuning the atomic arrangement and coordination of the outer atoms [18]; (iv) the 'anchor effect' of Co to Pt [13].

To show the electrochemical stability of the Pt-CoSn/C and PtSn/C catalysts for ethanol oxidation, CV cycling was carried out in 0.5 M CH_3CH_2OH + 0.5 M H_2SO_4 solution, as shown in Fig. 4. It can be seen that the loss of the electrocatalytic activity for Pt-CoSn/C is lower than those of the Pt/C and PtSn/C catalysts, further indicating that the present Pt-CoSn/C has good stability. This maybe attributed to CoSn alloys are in the amorphous state [15].

4. Conclusions

In this article, a two-stage method was used to prepare carbon supported Pt decorating amorphous CoSn alloy with mean particle size of 2.3 nm. The mass activity of the Pt-CoSn/C catalyst is 454.6 mA mg^{-1} Pt, which is about 1.71 and 1.74 times those of Pt/C (266.2 mA mg^{-1} Pt) and PtSn/C (261.2 mA mg^{-1} Pt) catalysts respectively. The better electrocatalytic activity of the Pt-CoSn/C catalyst can be attributed to it being an amorphous alloys and its modified electronic structure. These encouraging findings could be expanded to other amorphous electrocatalysts and open up a new direction of electrocatalysts.

Acknowledgements

The State Natural Science Foundation of China (20774074), the Key Project of Ministry of Education Foundation of China (209129) and the Scientific and Technical Innovation Project of Northwest Normal University (NWNU-kjcxgc-03-63) are financially supporting this work.

References

[1] F. Colmati, E. Antolini, E.R. Gonzalez, Appl. Catal. B: Environ. 73 (2007) 106.
[2] Z.B. Wang, G.P. Yin, J. Zhang, Y.C. Sun, P.F. Shi, Electrochim. Acta 51 (2006) 5691.
[3] W.Z. Li, X. Wang, Z.W. Chen, M. Waje, Y.S. Yan, J. Phys. Chem. B 110 (2006) 15353.
[4] C.T. Hsieh, J.Y. Lin, J. Power Sources 188 (2009) 347.
[5] Y. Ishikawa, M.S. Liao, C.R. Cabrera, Surf. Sci. 463 (2000) 66.
[6] E. Antolini, E.R. Gonzalez, Catal. Today 160 (2011) 28.
[7] F. Colmati, E. Antolini, E.R. Gonzalez, Electrochim. Acta 50 (2005) 5496.
[8] I. Honma, T. Toda, J. Electrochem. Soc. 150 (2003) A1689.
[9] E.E. Switzer, T.S. Olson, A.K. Datye, P. Atanassov, M.R. Hibbs, C.J. Cornelius, Electrochim. Acta 54 (2009) 989.
[10] L. Jiang, G. Sun, Sh. Sun, J. Liu, S. Tang, H. Li, B. Zhou, Q. Xin, Electrochim. Acta 50 (2005) 5384.
[11] L. Jiang, A. Hsu, D. Chu, R. Chen, Int. J. Hydrogen Energy 35 (2010) 365.
[12] S.S. Gupta, S. Singh, J. Datta, Mater. Chem. Phys. 116 (2009) 223.
[13] A.V. Tripković, K.D. Popović, J.D. Lović, V.M. Jovanović, S.I. Stevanović, D.V. Tripković, A. Kowal, Electrochem. Commun. 11 (2009) 1030.
[14] M. Stacheva, St. Manev, D. Lazarov, J. Alloys Compd. 234 (1996) 251–255.
[15] K. Hashimoto, Appl. Sur. Sci. doi:10.1016/j.apsusc.2010.12.142.
[16] Q. Han, K. Liu, J. Chen, X. Li, X. Wei, Int. J. Hydrogen Energy 29 (2004) 243.
[17] T.C. Blanco, A.R. Pierna, J. Barroso, J. Power Sources 196 (2011) 4337.
[18] X.B. Zhang, J.M. Yan, S. Han, H. Shioyama, Q. Xu, J. Am. Chem. Soc. 131 (2009) 2778.
[19] Z. Peng, H. You, H. Yang, Adv. Funct. Mater. 20 (2010) 3734.
[20] X.Z. Fu, Y. Liang, S.P. Chen, J.D. Lin, D.W. Liao, Catal. Commun. 10 (2009) 1893.
[21] R.F. Wang, H. Wang, B.X. Wei, W. Wang, Z.Q. Lei, Int. J. Hydrogen Energy 35 (2010) 10081.
[22] S. Koh, C. Yu, Pr. Mani, R. Srivastava, P. Strasser, J. Power Sources 172 (2007) 50.
[23] X. Zhang, H. Zhu, Z. Guo, Y. Wei, F. Wang, Int. J. Hydrogen Energy 35 (2010) 8841.
[24] R.F. Wang, H. Li, S. Ji, H. Wang, Z.Q. Lei, Electrochim. Acta 55 (2010) 1519.
[25] M. Arenz, V. Stamenković, B.B. Blizanac, K.J. Mayrhofer, N.M. Marković, P.N. Ross, J. Catal. 232 (2005) 402.
[26] T.E. Shubina, M.T.M. Koper, Electrochim. Acta 47 (2002) 3621.